

## 2-[1-(2,6-Dibenzhydryl-4-chlorophenylimino)ethyl]-6-[1-(arylimino)ethyl]pyridyliron(II) dichlorides: Synthesis, characterization and ethylene polymerization behavior

Xiaoping Cao<sup>a</sup>, Fan He<sup>a,b</sup>, Weizhen Zhao<sup>b</sup>, Zhengguo Cai<sup>c</sup>, Xiang Hao<sup>b</sup>, Takeshi Shiono<sup>c</sup>, Carl Redshaw<sup>d,\*\*</sup>, Wen-Hua Sun<sup>a,b,\*</sup>

<sup>a</sup> State Key Laboratory of Applied Organic Chemistry, College of Chemistry and Chemical Engineering, Lanzhou University, Lanzhou 730000, China

<sup>b</sup> Key Laboratory of Engineering Plastics, Beijing National Laboratory for Molecular Sciences, Institute of Chemistry, Chinese Academy of Sciences, Beijing 100190, China

<sup>c</sup> Department of Applied Chemistry, Hiroshima University, Higashi-Hiroshima 739-8527, Japan

<sup>d</sup> School of Chemistry, University of East Anglia, Norwich NR4 7TJ, UK

### ARTICLE INFO

#### Article history:

Received 8 December 2011

Received in revised form

17 February 2012

Accepted 27 February 2012

Available online 3 March 2012

#### Keywords:

Ethylene polymerization

Linear polyethylene

Iron pre-catalysts

### ABSTRACT

A series of 2-[1-(2,6-dibenzhydryl-4-chlorophenylimino)ethyl]-6-[1-(arylimino)ethyl]pyridine ligands (**L1**–**L5**) as well as the ligand 2,6-bis[1-(2,6-dibenzhydryl-4-chloro-phenylimino)ethyl]pyridine (**L6**) were synthesized and reacted with  $\text{FeCl}_2 \cdot 4\text{H}_2\text{O}$  to afford the iron(II) dichloride complexes [ $\text{LFeCl}_2$ ] (**Fe1**–**Fe6**). All new compounds were fully characterized by elemental and spectroscopic analysis, and the molecular structures of the complexes **Fe1**, **Fe2** and **Fe4** were determined by single-crystal X-ray diffraction, which revealed a pseudo-square-pyramidal geometry at iron. Upon activation with either MAO or MMAO, all iron pre-catalysts exhibited very high activity in ethylene polymerization with good thermal stability. To the best of our knowledge, the current system showed the highest activity amongst iron bis(imino)pyridine pre-catalysts reported to-date. The polymerization parameters were explored to determine the optimum conditions for catalytic activity, which were typically found to be 2500 eq. Al to Fe at 60 °C in the presence of MMAO, and 80 °C in the presence of MAO. The resultant polyethylene possessed a narrow molecular polydispersity index (PDI) consistent with the formation of single-site active species.

© 2012 Elsevier Ltd. All rights reserved.

### 1. Introduction

The discovery of bis(imino)pyridyliron(II) chloride pre-catalysts in ethylene polymerization was a relatively recent milestone within polyolefin science [1,2]. Subsequently, extensive research has focused on the derivatization of such pre-catalysts via the variation of the substituents on the framework of the parent bis(imino)pyridine ligand set [3–18]. Moreover, there have been a number of investigations into new, but related iron pre-catalysts which employ  $\text{sp}^2$ -nitrogen-donating tridentate ligand sets such as 6-benzimidazolyl-2-iminopyridines [19–21], 6-benzoxazolyl-2-iminopyridines [22,23], 2-quinoxalyl-6-iminopyridines [24], 2-imino-1,10-phenanthrolines [25–27], 2-(2-benzimidazolyl)-1,10-

phenanthrolines [28], 2-(benzoxazolyl)-1,10-phenanthrolines [29], 2,8-bis(1-aryliminoethyl)quinolines [30], *N*-((pyridin-2-yl)methylene)-8-amino-quinolines [31], 8-(1*H*-benzimidazol-2-yl)quinolines [32], and a few reports involving bidentate ligands such as 8-benzimidazolylquinoline [33,34] and 8-iminoquinaldine ligands [35]. Although high catalytic activities have been achieved for most of these iron pre-catalyst systems, as reported in a number of recent review articles [36–42], the critical problems of catalyst deactivation together with the formation of low molecular weight products at elevated reaction temperature, have not been overcome. Using knowledge accumulated for the numerous models of iron pre-catalysts, it should be possible to address these problematic issues to enable such iron-based catalysts to be more suited for industrial applications.

Ethylene polymerization is a highly exothermic reaction, and the industrial process prefers the polymerization to be conducted at temperatures between 60 and 90 °C. Given this, the catalytic system should remain highly active at such high reaction temperatures. Furthermore, it is desirable for the catalytic system to produce polyethylene waxes with narrow PDIs, which are both very

\* Corresponding author. Key Laboratory of Engineering Plastics, Beijing National Laboratory for Molecular Sciences, Institute of Chemistry, Chinese Academy of Sciences, Beijing 100190, China. Tel.: +86 10 62557955; fax: +86 10 62618239.

\*\* Corresponding author.

E-mail addresses: [Carl.Redshaw@uea.ac.uk](mailto:Carl.Redshaw@uea.ac.uk) (C. Redshaw), [whsun@iccas.ac.cn](mailto:whsun@iccas.ac.cn) (W.-H. Sun).

useful and often of greater commercial value than the common polyethylenes. Having these required catalytic features in mind, there are only a limited number of papers relating to iron pre-catalysts ligated by 2,8-bis(1-aryliminoethyl)quinolines [30], 8-benzimidazolylquinolines [33,34] and unsymmetrical bis(imino)pyridines bearing extremely bulky substituents [43–46]. However, the extensive use of bis(imino)pyridines possessing bulky substituents has not been widely explored, basically due to the rather limited number of commercially available bulky anilines. Encouraged by the success of the 2-[1-(2,6-dibenzhydryl-4-methylphenylimino)ethyl]-6-[1-(arylimino)ethyl]pyridyliron(II) pre-catalyst system [43], which, for this type of pre-catalyst, performed with the highest observed activity in ethylene polymerization reported at that time (we note however that such high activities are usually achieved in the presence of large amounts of alkylaluminum co-catalyst), iron pre-catalysts bearing 2-[1-(2,6-dibenzhydryl-4-methylphenylimino)ethyl]-6-[1-(arylimino)ethyl]pyridines were synthesized and revealed higher catalytic activities for ethylene polymerization [45]. Noting the enhanced catalytic activities of iron pre-catalysts bearing ligands with electron-withdrawing groups, 2,6-dibenzhydryl-4-chloroaniline was prepared and was subsequently used to form a new family of 2-[1-(2,6-dibenzhydryl-4-chloro-phenylimino)ethyl]-6-[1-(arylimino)ethyl]pyridine ligands. The title iron chloride complexes were readily formed and were investigated for their catalytic behavior toward ethylene polymerization. To the best of our knowledge, the iron pre-catalysts possess the highest catalytic activities for ethylene polymerization reported to-date for bis(imino)pyridine containing pre-catalysts. Moreover, they afforded polyethylene with the narrowest PDIs in the family of unsymmetrical bis(imino)pyridines bearing extremely bulky substituents, indicative of a single-site catalytic system. Herein, the synthesis, characterization, and catalytic behavior of the 2-[1-(2,6-dibenzhydryl-4-chlorophenylimino)ethyl]-6-[1-(arylimino)ethyl]pyridyliron(II) complexes are reported and discussed in detail.

## 2. Experimental

### 2.1. General considerations

All manipulations of air and moisture-sensitive compounds were performed under a nitrogen atmosphere using standard Schlenk techniques. Toluene was refluxed over sodium-benzophenone and distilled under nitrogen prior to use. Methylaluminoxane (MAO, a 1.46 M solution in toluene) and modified methylaluminoxane (MMAO, 1.93 M in heptane, 3A) were purchased from Akzo Nobel Corp. Other reagents were purchased from Acros Chemicals or local suppliers.  $^1\text{H}$  and  $^{13}\text{C}$  NMR spectra of compounds and PE samples were recorded on Bruker DMX 400 MHz instrument at ambient temperature using TMS as an internal standard. IR spectra were recorded on a Perkin–Elmer System 2000 FT-IR spectrometer. Elemental analysis was carried out using a Flash EA 1112 micro analyzer. Molecular weights and polydispersity index of the polyethylenes were determined by a PL-GPC220 at 150 °C, with 1,2,4-trichlorobenzene as the solvent. DSC trace and melting points of polyethylenes were obtained from the second scanning run on Perkin–Elmer DSC-7 at a heating rate of 10 °C/min.

### 2.2. Synthesis and characterization

#### 2.2.1. Synthesis of 2-acetyl-6-[1-(2,6-dibenzhydryl-4-chlorophenylimino)ethyl]pyridine and 2,6-bis[1-(2,6-dibenzhydryl-4-chlorophenylimino)ethyl]pyridine (**L6**)

A solution of 2,6-dibenzhydryl-4-chlorophenylamine (4.60 g, 10.0 mmol), 2,6-diacetylpyridine (1.63 g, 10.0 mmol) and

a catalytic amount of *p*-toluenesulfonic acid in toluene (125 mL) was refluxed for 4 h. After removing the solvent in vacuo, the crude product was purified by silica gel column chromatography (30:1 (v/v) petroleum ether/ethyl acetate) to afford 3.15 g (52%) of 2-acetyl-6-[1-(2,6-dibenzhydryl-4-chlorophenylimino)ethyl]pyridine as a yellow powder and 2.09 g of **L6** (20%) as a white powder. Data for 2-acetyl-6-[1-(2,6-dibenzhydryl-4-chlorophenylimino)ethyl]pyridine: Mp: 156–158 °C. FT-IR (KBr,  $\text{cm}^{-1}$ ): 3027, 2920, 2170, 1700, 1650 ( $\nu_{\text{C}=\text{N}}$ ), 1494, 1446, 1360, 1240, 1118, 1076, 1029, 819, 761, 738, 700.  $^1\text{H}$  NMR (400 MHz,  $\text{CDCl}_3$ , TMS):  $\delta$  8.14 (d,  $J = 7.8$  Hz, 1H, Py- $H_m$ ), 8.10 (d,  $J = 7.6$  Hz, 1H, Py- $H_m$ ), 7.87 (t,  $J = 7.8$  Hz, 1H, Py- $H_p$ ), 7.29–7.13 (m, 12H, aryl- $H$ ), 7.00 (t,  $J = 8.0$  Hz, 8H, aryl- $H$ ), 6.87 (s, 2H, aryl- $H$ ), 5.24 (s, 2H,  $\text{CHPh}_2$ ), 2.66 (s, 3H,  $\text{O}=\text{CCH}_3$ ), 1.06 (s, 3H,  $\text{N}=\text{CCH}_3$ ).  $^{13}\text{C}$  NMR (100 MHz,  $\text{CDCl}_3$ , TMS):  $\delta$  200.0, 170.0, 155.1, 152.4, 146.9, 142.7, 141.7, 137.3, 134.5, 129.8, 129.4, 128.8, 128.6, 128.4, 128.1, 127.0, 126.6, 126.5, 124.7, 122.6, 52.3, 25.7, 17.0. Anal. Calcd for  $\text{C}_{41}\text{H}_{33}\text{ClN}_2\text{O}$  (605.17): C, 80.99; H, 5.68; N, 4.48. Found: C, 81.37; H, 5.50; N, 4.63. Data for **L6**: Mp: 270–272 °C. FT-IR (KBr,  $\text{cm}^{-1}$ ): 3058, 3025, 1974, 1638 ( $\nu_{\text{C}=\text{N}}$ ), 1493, 1446, 1369, 1242, 766, 743, 698.  $^1\text{H}$  NMR (400 MHz,  $\text{CDCl}_3$ , TMS):  $\delta$  8.10 (d,  $J = 7.8$  Hz, 2H, Py- $H_m$ ), 7.80 (t,  $J = 7.8$  Hz, 1H, Py- $H_p$ ), 7.30–7.09 (m, 24H, aryl- $H$ ), 7.04–6.99 (m, 16H, aryl- $H$ ), 6.88 (s, 4H, aryl- $H$ ), 5.28 (s, 4H,  $\text{CHPh}_2$ ), 0.91 (s, 6H,  $\text{N}=\text{CCH}_3$ ).  $^{13}\text{C}$  NMR (100 MHz,  $\text{CDCl}_3$ , TMS):  $\delta$  170.7, 154.6, 147.0, 142.9, 141.8, 136.7, 134.5, 129.8, 129.4, 128.6, 128.3, 128.2, 128.1, 126.5, 122.3, 52.1, 17.0. Anal. Calcd for  $\text{C}_{73}\text{H}_{57}\text{Cl}_2\text{N}_3$  (1047.16): C, 83.31, H, 5.69; N, 3.88. Found: C, 83.73; H, 5.49; N, 4.01.

#### 2.2.2. Synthesis of 2-[1-(2,6-dibenzhydryl-4-chlorophenylimino)ethyl]-6-[1-(arylimino)ethyl]pyridine (**L1–L5**)

2.2.2.1. 2-[1-(2,6-dibenzhydryl-4-chlorophenylimino)ethyl]-6-[1-(2,6-dimethylphenylimino)ethyl]pyridine (**L1**). A mixture of 2-acetyl-6-[1-(2,6-dibenzhydryl-4-chlorophenylimino)ethyl]pyridine (3.02 g, 5.0 mmol), 2,6-dimethylaniline (0.91 g, 7.5 mmol) and a catalytic amount of *p*-toluenesulfonic acid in toluene (50 mL) was refluxed for 8 h. The solution was evaporated in vacuo and the residual solid was purified by silica gel column chromatography (30:1 (v/v) petroleum ether/ethyl acetate) to afford 1.93 g (55%) of **L1** as a yellow powder. Mp: 222–223 °C. FT-IR (KBr,  $\text{cm}^{-1}$ ): 3057, 3023, 2916, 2361, 2161, 2034, 1639 ( $\nu_{\text{C}=\text{N}}$ ), 1494, 1448, 1365, 1242, 1120, 1076, 1032, 762, 699.  $^1\text{H}$  NMR (400 MHz,  $\text{CDCl}_3$ , TMS):  $\delta$  8.42 (d,  $J = 7.7$  Hz, 1H, Py- $H_m$ ), 8.02 (d,  $J = 7.7$  Hz, 1H, Py- $H_m$ ), 7.84 (t,  $J = 7.8$  Hz, 1H, Py- $H_p$ ), 7.31–7.11 (m, 12H, aryl- $H$ ), 7.08 (d,  $J = 7.5$  Hz, 2H, aryl- $H$ ), 7.02 (t,  $J = 7.2$  Hz, 8H, aryl- $H$ ), 6.95 (t,  $J = 7.5$  Hz, 1H, aryl- $H$ ), 6.86 (s, 2H, aryl- $H$ ), 5.27 (s, 2H,  $\text{CHPh}_2$ ), 2.11 (s, 3H,  $\text{N}=\text{CCH}_3$ ), 2.06 (s, 6H, aryl- $\text{o}-\text{CH}_3$ ), 1.27 (s, 3H,  $\text{N}=\text{CCH}_3$ ).  $^{13}\text{C}$  NMR (100 MHz,  $\text{CDCl}_3$ , TMS):  $\delta$  170.4, 167.2, 155.0, 154.6, 148.7, 147.0, 142.7, 141.7, 136.7, 134.4, 129.8, 129.4, 128.5, 128.2, 128.0, 127.9, 126.4, 126.3, 125.4, 123.0, 122.3, 122.2, 52.1, 18.0, 17.0, 16.4. Anal. Calcd for  $\text{C}_{49}\text{H}_{42}\text{ClN}_3$  (708.33): C, 82.75; H, 6.10; N, 5.77. Found: C, 83.09; H, 5.98; N, 5.93.

2.2.2.2. 2-[1-(2,6-dibenzhydryl-4-chlorophenylimino)ethyl]-6-[1-(2,6-diethylphenylimino)ethyl]pyridine (**L2**). A procedure similar to that for **L1** was used, but using 3.02 g (5.0 mmol) of 2-acetyl-6-[1-(2,6-dibenzhydryl-4-chlorophenylimino)ethyl]pyridine and 1.12 g (7.5 mmol) of 2,6-diethylaniline, to afford 1.75 g (48%) of **L2** as a yellow powder. Mp: 202–203 °C. FT-IR (KBr,  $\text{cm}^{-1}$ ): 3024, 2963, 2868, 2170, 2033, 1974, 1639 ( $\nu_{\text{C}=\text{N}}$ ), 1494, 1448, 1366, 1233, 1120, 1074, 764, 699.  $^1\text{H}$  NMR (400 MHz,  $\text{CDCl}_3$ , TMS):  $\delta$  8.41 (d,  $J = 7.8$  Hz, 1H, Py- $H_m$ ), 8.03 (d,  $J = 7.8$  Hz, 1H, Py- $H_m$ ), 7.84 (t,  $J = 7.8$  Hz, 1H, Py- $H_p$ ), 7.30–7.15 (m, 12H, aryl- $H$ ), 7.13 (d,  $J = 7.5$  Hz, 2H, aryl- $H$ ), 7.03 (m, 9H, aryl- $H$ ), 6.87 (s, 2H, aryl- $H$ ), 5.28 (s, 2H,  $\text{CHPh}_2$ ), 2.40 (m, 4H,  $\text{CH}_2\text{CH}_3$ ), 2.12 (s, 3H,  $\text{N}=\text{CCH}_3$ ), 1.16 (m, 9H,  $\text{CH}_3$ ).  $^{13}\text{C}$  NMR (100 MHz,  $\text{CDCl}_3$ , TMS):  $\delta$  170.6, 167.1, 155.2, 154.8,

147.9, 147.1, 142.8, 141.9, 136.8, 134.5, 131.3, 130.0, 129.5, 128.6, 128.4, 128.2, 128.1, 126.6, 126.1, 123.5, 122.4, 122.3, 52.2, 24.7, 17.2, 16.9, 13.9. Anal. Calcd for  $C_{51}H_{46}ClN_3$  (736.38): C, 82.97, H, 6.62; N, 5.68. Found: C, 83.18; H, 6.30; N, 5.71.

**2.2.2.3. 2-[1-(2,6-dibenzhydryl-4-chlorophenylimino)ethyl]-6-[1-(2,6-diisopropylphenylimino)ethyl]pyridine (L3).** A procedure similar to that for **L1** was used, but using 3.02 g (5.0 mmol) of 2-acetyl-6-[1-(2,6-dibenzhydryl-4-chlorophenylimino)ethyl]pyridine and 1.33 g (7.5 mmol) of 2,6-diisopropylaniline, to afford 1.72 g (45%) of **L3** as a yellow powder. Mp: 179–180 °C. FT-IR (KBr,  $cm^{-1}$ ): 3062, 3027, 2958, 2167, 1636 ( $\nu_{C=N}$ ), 1495, 1432, 1369, 1235, 1126, 823, 767, 699.  $^1H$  NMR (400 MHz,  $CDCl_3$ , TMS):  $\delta$  8.39 (d,  $J = 7.8$  Hz, 1H, Py- $H_m$ ), 8.02 (d,  $J = 7.8$  Hz, 1H, Py- $H_m$ ), 7.84 (t,  $J = 7.7$  Hz, 1H, Py- $H_p$ ), 7.30–7.08 (m, 15H, aryl- $H$ ), 7.02 (t, 8H,  $J = 8.0$  Hz, aryl- $H$ ), 6.87 (s, 2H, aryl- $H$ ), 5.28 (s, 2H,  $CHPh_2$ ), 2.77 (m, 2H,  $CHMe_2$ ), 2.13 (s, 3H,  $N=CCH_3$ ), 1.18 (d,  $J = 6.7$  Hz, 12H,  $CH_3$ ), 1.14 (s, 3H,  $N=CCH_3$ ).  $^{13}C$  NMR (100 MHz,  $CDCl_3$ , TMS):  $\delta$  170.6, 167.1, 155.1, 154.8, 147.1, 146.5, 142.8, 141.8, 136.8, 135.9, 134.5, 129.9, 129.4, 128.5, 128.3, 128.1, 128.1, 126.5, 126.5, 123.75, 123.11, 122.4, 122.3, 52.2, 28.4, 23.4, 23.0, 17.2, 17.1. Anal. Calcd for  $C_{53}H_{50}ClN_3$  (764.44): C, 83.02, H, 7.03; N, 5.35. Found: C, 83.27; H, 6.59; N, 5.50.

**2.2.2.4. 2-[1-(2,6-dibenzhydryl-4-chlorophenylimino)ethyl]-6-[1-(2,4,6-trimethylphenylimino)ethyl]pyridine (L4).** A procedure similar to that for **L1** was used, but using 3.02 g (5.0 mmol) of 2-acetyl-6-[1-(2,6-dibenzhydryl-4-chlorophenylimino)ethyl]pyridine and 1.01 g (7.5 mmol) of 2,4,6-trimethylaniline, to afford 1.51 g (45%) of **L4** as a yellow powder. Mp: 228–229 °C. FT-IR (KBr,  $cm^{-1}$ ): 3060, 3025, 2914, 1943, 1643 ( $\nu_{C=N}$ ), 1493, 1431, 1365, 1216, 1122, 740, 698.  $^1H$  NMR (400 MHz,  $CDCl_3$ , TMS):  $\delta$  8.41 (d,  $J = 7.8$  Hz, 1H, Py- $H_m$ ), 8.02 (d,  $J = 7.8$  Hz, 1H, Py- $H_m$ ), 7.82 (t,  $J = 7.8$  Hz, 1H, Py- $H_p$ ), 7.33–7.12 (m, 12H, aryl- $H$ ), 7.02 (t, 8H,  $J = 7.6$  Hz, aryl- $H$ ), 6.90 (s, 2H, aryl- $H$ ), 6.86 (s, 2H, aryl- $H$ ), 5.27 (s, 2H,  $CHPh_2$ ), 2.30 (s, 3H, aryl- $p-CH_3$ ), 2.10 (s, 3H,  $N=CCH_3$ ), 2.02 (s, 6H, aryl- $o-CH_3$ ), 1.11 (s, 3H,  $N=CCH_3$ ).  $^{13}C$  NMR (100 MHz,  $CDCl_3$ , TMS):  $\delta$  170.5, 167.4, 155.1, 154.6, 147.0, 146.2, 141.7, 136.7, 134.4, 132.2, 129.8, 129.4, 128.6, 128.5, 128.2, 128.0, 126.4, 126.3, 125.2, 122.2, 122.1, 52.1, 20.7, 17.9, 17.0, 16.3. Anal. Calcd for  $C_{50}H_{44}ClN_3$  (722.36): C, 82.86, H, 6.44; N, 5.63. Found: C, 83.14; H, 6.14; N, 5.82.

**2.2.2.5. 2-[1-(2,6-dibenzhydryl-4-chlorophenylimino)ethyl]-6-[1-(2,6-diethyl-4-methylphenylimino)ethyl]pyridine (L5).** A procedure similar to that for **L1** was used, but using 3.02 g (5.0 mmol) of 2-acetyl-6-[1-(2,6-dibenzhydryl-4-chlorophenylimino)ethyl]pyridine and 1.22 g (7.5 mmol) of 2,6-diethyl-4-methylaniline, to afford 1.77 g (47%) of **L5** as a yellow powder. Mp: 211–212 °C. FT-IR (KBr,  $cm^{-1}$ ): 3060, 3026, 2964, 2170, 1943, 1639 ( $\nu_{C=N}$ ), 1494, 1447, 1364, 1211, 1121, 860, 740, 698.  $^1H$  NMR (400 MHz,  $CDCl_3$ , TMS):  $\delta$  8.39 (d,  $J = 7.8$  Hz, 1H, Py- $H_m$ ), 8.02 (d,  $J = 7.8$  Hz, 1H, Py- $H_m$ ), 7.82 (t,  $J = 7.8$  Hz, 1H, Py- $H_p$ ), 7.30–7.12 (m, 12H, aryl- $H$ ), 7.02 (t, 8H,  $J = 8.1$  Hz, aryl- $H$ ), 6.94 (s, 2H, aryl- $H$ ), 6.86 (s, 2H, aryl- $H$ ), 5.27 (s, 2H,  $CHPh_2$ ), 2.35 (m, 4H,  $CH_2CH_3$ ), 2.34 (s, 3H, aryl- $p-CH_3$ ), 2.11 (s, 3H,  $N=CCH_3$ ), 1.14 (m, 9H,  $CH_3$ ).  $^{13}C$  NMR (100 MHz,  $CDCl_3$ , TMS):  $\delta$  170.6, 167.1, 155.2, 154.8, 147.9, 147.1, 142.8, 141.9, 136.8, 134.5, 131.3, 129.9, 129.5, 128.6, 128.4, 128.2, 128.1, 126.6, 123.5, 122.4, 122.3, 52.2, 24.7, 17.2, 16.9, 13.9. Anal. Calcd for  $C_{52}H_{48}ClN_3$  (750.41): C, 82.80, H, 6.78; N, 5.46. Found: C, 83.23; H, 6.45; N, 5.60.

### 2.2.3. Synthesis of iron complexes (Fe1–Fe6)

To the corresponding ligand, 1.0 equivalents of  $FeCl_2 \cdot 4H_2O$  and freshly distilled ethanol were added in a Schlenk tube. A blue precipitate was formed while this reaction mixture was stirred at

room temperature for 8 h, which was then filtered and washed with diethyl ether ( $3 \times 5$  mL). The pure complex was obtained as a blue powder after drying under vacuo.

Complex **Fe1** was prepared in 88% yield. FT-IR (KBr,  $cm^{-1}$ ): 3059, 3025, 2968, 2168, 1977, 1582 ( $\nu_{C=N}$ ), 1495, 1431, 1364, 1267, 1214, 1077, 1031, 813, 767, 743, 699. Anal. Calcd for  $C_{49}H_{42}Cl_3FeN_3$  (835.08): C, 70.02; H, 5.45; N, 4.86. Found: C, 70.48; H, 5.07; N, 5.03. Complex **Fe2** was prepared in 92% yield. FT-IR (KBr,  $cm^{-1}$ ): 3061, 3026, 2966, 2915, 2165, 1977, 1580 ( $\nu_{C=N}$ ), 1495, 1434, 1366, 1268, 1208, 1076, 1031, 810, 769, 743, 700. Anal. Calcd for  $C_{51}H_{46}Cl_3FeN_3$  (863.14): C, 70.61; H, 5.86; N, 4.69. Found: C, 70.97; H, 5.37; N, 4.87. Complex **Fe3** was prepared in 87% yield. FT-IR (KBr,  $cm^{-1}$ ): 3060, 3027, 2959, 2913, 2165, 2077, 1579 ( $\nu_{C=N}$ ), 1496, 1434, 1370, 1268, 1207, 1028, 808, 770, 751, 702. Anal. Calcd for  $C_{53}H_{50}Cl_3FeN_3$  (891.19): C, 71.08; H, 5.93; N, 4.53. Found: C, 71.43; H, 5.66; N, 4.72. Complex **Fe4** was prepared in 84% yield. FT-IR (KBr,  $cm^{-1}$ ): 3063, 3032, 2970, 2918, 2168, 1980, 1581 ( $\nu_{C=N}$ ), 1495, 1430, 1363, 1267, 1221, 1077, 1030, 767, 700. Anal. Calcd for  $C_{50}H_{44}Cl_3FeN_3$  (849.11): C, 70.42; H, 5.57; N, 4.77. Found: C, 70.73; H, 5.22; N, 4.95. Complex **Fe5** was prepared in 86% yield. FT-IR (KBr,  $cm^{-1}$ ): 3062, 3030, 2960, 2915, 2165, 1978, 1581 ( $\nu_{C=N}$ ), 1496, 1445, 1373, 1267, 1217, 1033, 870, 807, 767, 704. Anal. Calcd for  $C_{52}H_{48}Cl_3FeN_3$  (877.16): C, 70.83; H, 5.80; N, 4.65. Found: C, 71.20; H, 5.52; N, 4.79. Complex **Fe6** was prepared in 70% yield. FT-IR (KBr,  $cm^{-1}$ ): 3026, 2168, 1978, 1575 ( $\nu_{C=N}$ ), 1494, 1433, 1269, 1203, 1075, 1030, 808, 766, 700. Anal. Calcd for  $C_{73}H_{57}Cl_4FeN_3$  (1173.91): C, 74.22; H, 5.23; N, 3.33. Found: C, 74.69; H, 4.89; N, 3.58.

### 2.3. X-ray crystallographic studies

Single-crystal X-ray diffraction studies for **Fe1**, **Fe2** and **Fe4** were carried out on a Rigaku Saturn724 + CCD diffractometer with graphite-monochromated Mo  $K\alpha$  radiation ( $\lambda = 0.71073$  Å) at 173 (2) K. Cell parameters were obtained by global refinement of the positions of all collected reflections. Intensities were corrected for Lorentz and polarization effects and empirical absorption. The structures were solved by direct methods and refined by full-matrix least-squares on  $F^2$ . All non-hydrogen atoms were refined anisotropically. The hydrogen atoms were placed in calculated positions. Structure solution and refinement were performed by using the SHELXL-97 package [47]. Crystal data and processing parameters for **Fe1**, **Fe2** and **Fe4** are summarized in Table 1.

### 2.4. General procedure for ethylene polymerization

#### 2.4.1. Ethylene polymerization at ambient pressure

The pre-catalyst was dissolved in toluene using standard Schlenk techniques, and the reaction solution was stirred with a magnetic stir bar under ethylene atmosphere (1 atm) with a steam bath for controlling the desired temperature. Finally, the require amount of co-catalyst (MMAO) was added by a syringe. After the reaction was carried out for the required period, the reaction solution was quenched with acidified ethanol solution containing 10% hydrochloric acid. The precipitated polymer was collected by filtration, washed with ethanol and water, and dried in a vacuum at 60 °C until of constant weight.

#### 2.4.2. Ethylene polymerization at 10 atm pressure

A 250 mL stainless steel autoclave, equipped with a mechanical stirrer and a temperature controller, was employed for the reaction. Firstly, 50 mL toluene (freshly distilled) was injected into the autoclave which was full of ethylene. Then 30 mL toluene solution of the complex (1.5  $\mu$ mol), the require amount of co-catalyst (MAO, MMAO) and 20 mL toluene were added by syringe successively

**Table 1**  
Crystal data and structure refinement for **Fe1**, **Fe2** and **Fe4**.

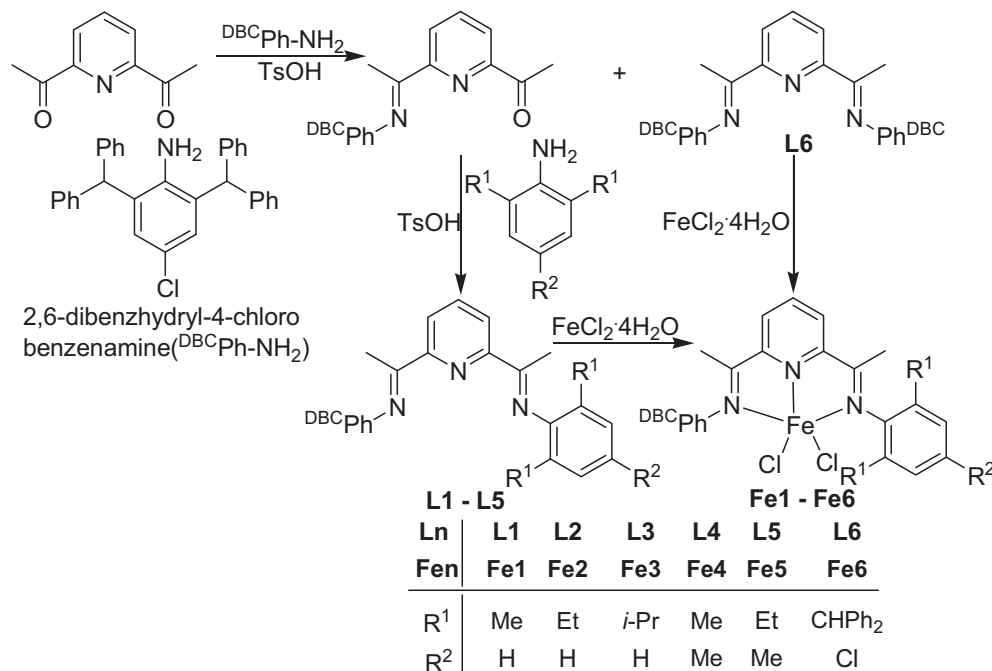
	<b>Fe1</b>	<b>Fe2</b>	<b>Fe4</b>
Empirical formula	C <sub>49</sub> H <sub>42</sub> Cl <sub>3</sub> FeN <sub>3</sub>	C <sub>51</sub> H <sub>46</sub> Cl <sub>3</sub> FeN <sub>3</sub>	C <sub>50</sub> H <sub>45</sub> Cl <sub>3</sub> FeN <sub>3</sub>
Fw	835.06	863.11	850.09
T (K)	173(2)	173(2)	173(2)
Wavelength (Å)	0.71073	0.71073	0.71073
Crystal system	Monoclinic	Monoclinic	Monoclinic
Space group	Cc	Cc	Cc
a (Å)	24.024(5)	23.941(5)	24.125(5)
b (Å)	14.396(3)	14.652(3)	14.632(3)
c (Å)	15.970(3)	15.929(3)	16.093(3)
α (°)	90	90	90
β (°)	125.06(3)	123.57(3)	126.62(3)
γ (°)	90	90	90
V (Å <sup>3</sup> )	4520.8(16)	4655.7(16)	4559.8(16)
Z	4	4	4
D calcd. (g cm <sup>-3</sup> )	1.227	1.231	1.238
μ (mm <sup>-1</sup> )	0.546	0.533	0.543
F (000)	1736	1800	1772
Cryst size (mm)	0.29 × 0.13 × 0.08	0.24 × 0.20 × 0.12	0.36 × 0.12 × 0.11
θ range (°)	1.75–25.32	1.72–25.37	1.74–25.33
Limiting indices	–20 ≤ h ≤ 28 –16 ≤ k ≤ 17 –19 ≤ l ≤ 16	–27 ≤ h ≤ 28 –17 ≤ k ≤ 17 –19 ≤ l ≤ 9	–28 ≤ h ≤ 28 –16 ≤ k ≤ 16 –19 ≤ l ≤ 19
No. of rflns collected	11672	8704	12700
No. unique rflns [R (int)]	6206 (0.0497)	5093 (0.0406)	7019 (0.0523)
Completeness to θ (%)	99.8	99.1	98.6
Abs corr.	None	None	None
data/restraints/params	6206/2/505	5093/21/533	7019/2/514
Goodness of fit on F <sup>2</sup>	1.070	1.101	1.030
Final R indices [I > 2σ(I)]	R1 = 0.0747 wR2 = 0.1957	R1 = 0.0548 wR2 = 0.1459	R1 = 0.0756 wR2 = 0.1904
R indices (all data)	R1 = 0.0801 wR2 = 0.2020	R1 = 0.0582 wR2 = 0.1495	R1 = 0.0839 wR2 = 0.1983
Largest diff peak and hole (e Å <sup>-3</sup> )	0.643 and –0.455	0.442 and –0.435	0.566 and –0.502

after the autoclave was heated to the required reaction temperature. The reaction mixture was intensively stirred for the desired time under 10 atm pressure of ethylene through the entire experiment. The reaction was terminated and analyzed using the same method as above for ethylene polymerization at ambient pressure.

### 3. Result and discussion

#### 3.1. Synthesis and characterization of the ligands and complexes

Procedures for the preparation of the ligands and complexes are shown in Scheme 1. The ligand 2,6-bis[1-(2,6-dibenzhydryl-4-



**Scheme 1.** Synthesis of the ligands and iron complexes.

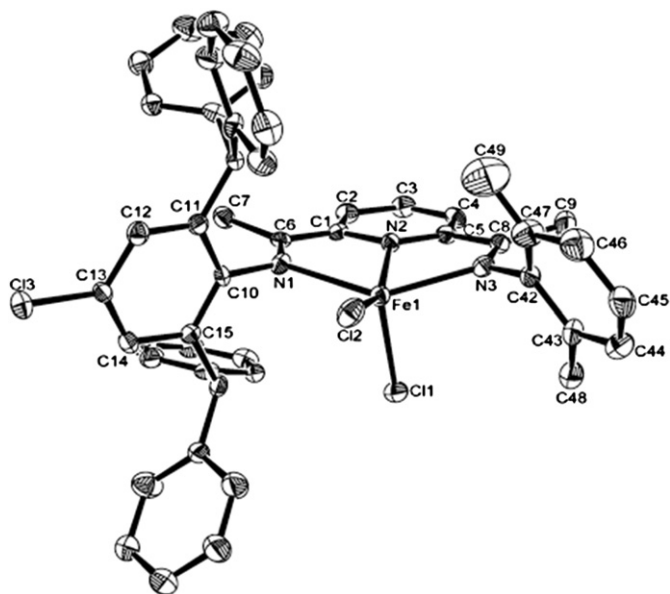


Fig. 1. Molecular structure of the complex **Fe1**; thermal ellipsoids are shown at 30% probability. Hydrogen atoms have been omitted for clarity.

chlorophenylimino)ethyl]pyridine (**L6**) was isolated as a by-product in the preparation of 2-acetyl-6-[1-(2,6-dibenzhydryl-4-chlorophenylimino)ethyl]pyridine, the latter being conveniently synthesized by the condensation of 2,6-diacetylpyridine with one equivalent of 2,6-dibenzhydryl-4-chlorophenylamine in refluxing toluene using a catalytic amount of *p*-toluenesulfonic acid. Further condensation of this product with the corresponding aniline produced the 2-[1-(2,6-dibenzhydryl-4-chlorophenylimino)ethyl]-6-[1-(arylimino)ethyl]pyridine ligands (**L1–L5**) in good yields. All ligands were fully characterized by elemental analysis,  $^1\text{H}$  and  $^{13}\text{C}$  NMR and FT-IR spectroscopy.

Reactions of ligands (**L1–L6**) with iron(II) dichloride afforded the iron complexes (**Fe1–Fe6**), which were characterized by FT-IR

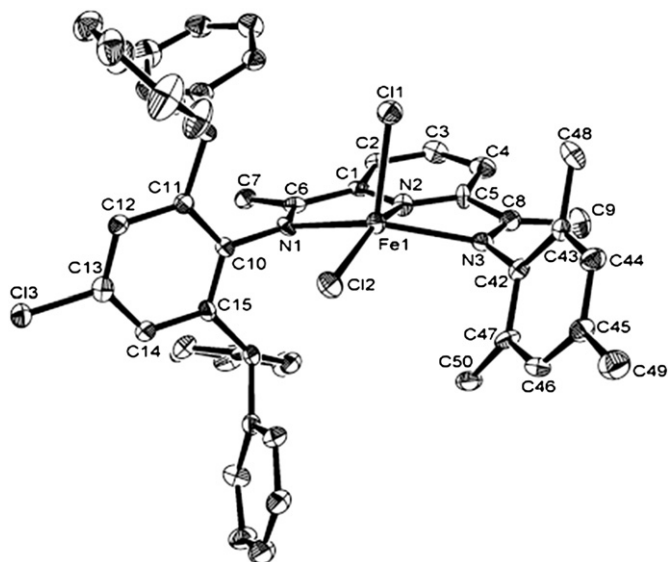


Fig. 3. Molecular structure of the complex **Fe4**; thermal ellipsoids are shown at 30% probability. Hydrogen atoms have been omitted for clarity.

spectroscopy and by elemental analysis. According to the FT-IR spectra, when compared with the corresponding free ligands ( $1636\text{--}1643\text{ cm}^{-1}$ ), the stretching vibrations for  $\text{C}=\text{N}$  in these complexes ( $1575\text{--}1582\text{ cm}^{-1}$ ) shifted to lower wave-numbers and the peak intensities were decreased, consistent with effective coordination between the imino-nitrogen and the cationic metal. The molecular structures of complexes **Fe1**, **Fe2** and **Fe4** were confirmed by single-crystal X-ray diffraction studies.

### 3.2. X-ray crystallographic studies

Single crystals of **Fe1**, **Fe2** and **Fe4** were grown by diffusing an *n*-hexane layer into dichloromethane solutions of the respective complexes. The molecular structures are shown in Figs. 1–3,

Table 2  
Selected bond lengths (Å) and angles ( $^\circ$ ) for complexes **Fe1**, **Fe2** and **Fe4**.

	<b>Fe1</b>	<b>Fe2</b>	<b>Fe4</b>
Bond lengths (Å)			
Fe1–N1	2.274 (6)	2.223 (4)	2.283 (6)
Fe1–N2	2.109 (5)	2.088 (5)	2.091 (6)
Fe1–N3	2.216 (6)	2.193 (5)	2.209 (6)
Fe1–Cl1	2.325 (2)	2.3264 (17)	2.331 (2)
Fe1–Cl2	2.266 (2)	2.2676 (19)	2.276 (2)
N1–C6	1.290 (9)	1.294 (7)	1.257 (9)
N1–Fe1 O	1.421 (9)	1.439 (7)	1.430 (8)
N2–Fe1	1.402 (9)	1.347 (7)	1.362 (9)
N2–C5	1.306 (9)	1.359 (7)	1.335 (8)
N3–C8	1.278 (9)	1.278 (8)	1.300 (10)
N3–C42	1.405 (9)	1.450 (7)	1.419 (9)
Bond angles ( $^\circ$ )			
N2–Fe1–N3	73.4 (2)	73.23 (19)	73.3 (2)
N2–Fe1–N1	72.4 (2)	72.15 (18)	72.0 (2)
N3–Fe1–N1	141.4 (2)	139.48 (18)	140.4 (2)
N2–Fe1–Cl2	154.61 (17)	155.48 (14)	155.68 (18)
N3–Fe1–Cl2	108.29 (16)	107.54 (14)	109.67 (17)
N1–Fe1–Cl2	95.29 (16)	95.72 (13)	94.78 (15)
N2–Fe1–Cl1	93.56 (16)	92.93 (13)	92.97 (18)
N3–Fe1–Cl1	94.76 (15)	96.21 (14)	93.72 (16)
N1–Fe1–Cl1	104.82 (15)	105.90 (12)	106.60 (15)
Cl2–Fe1–Cl1	111.27 (8)	111.10 (7)	110.59 (8)

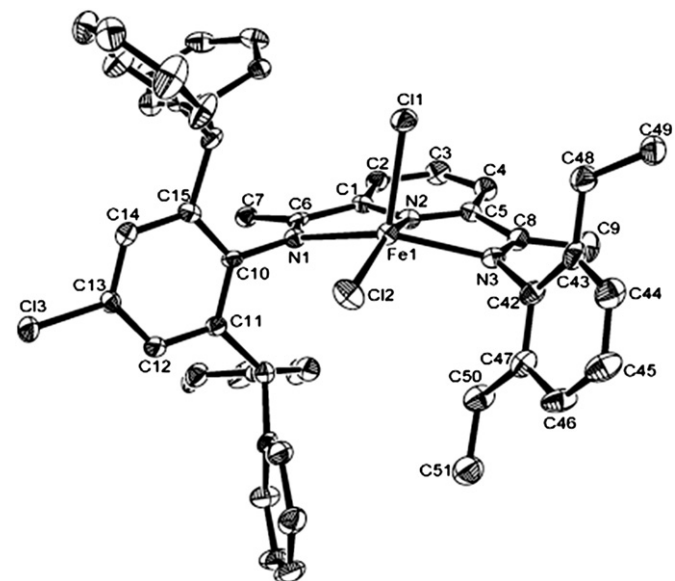


Fig. 2. Molecular structure of the complex **Fe2**; thermal ellipsoids are shown at 30% probability. Hydrogen atoms have been omitted for clarity.

**Table 3**  
Ethylene polymerization with **Fe1–Fe6**/MMAO.<sup>a</sup>

Run	Cat.	P/atm	T/°C	T/min	Al/Fe	Yield/g	Activity <sup>b</sup>	Adjusted activity <sup>c</sup>	M <sub>n</sub> <sup>d</sup> /10 <sup>4</sup> g mol <sup>-1</sup>	M <sub>w</sub> <sup>d</sup> /10 <sup>4</sup> g mol <sup>-1</sup>	M <sub>w</sub> /M <sub>n</sub> <sup>d</sup>	T <sub>m</sub> <sup>e</sup> /°C
1	<b>Fe4</b>	1	0	30	2500	1.09	1.45	7.22	0.29	7.0	24	129.7
2	<b>Fe4</b>	1	20	30	2500	0.89	1.19	8.18	0.21	0.76	3.6	124.7
3	<b>Fe4</b>	1	40	30	2500	0.86	1.15	10.5	0.11	0.34	3.1	119.9
4	<b>Fe4</b>	1	60	30	2500	0.53	0.71	8.28	0.13	0.23	1.8	106.4
5	<b>Fe4</b>	5	60	30	2500	7.73	2.06	24.0	0.48	3.0	6.3	127.0
6	<b>Fe4</b>	10	20	30	1500	2.08	0.28	1.90	5.8	120	21	134.7
7	<b>Fe4</b>	10	20	30	2000	2.62	0.35	2.40	1.1	38	35	133.7
8	<b>Fe4</b>	10	20	30	2500	2.81	0.38	2.58	2.1	9.5	4.5	131.2
9	<b>Fe4</b>	10	20	30	3000	2.64	0.35	2.42	0.65	1.1	1.7	122.4
10	<b>Fe4</b>	10	40	30	2500	3.54	0.47	4.30	1.1	7.3	6.6	132.5
11	<b>Fe4</b>	10	50	30	2500	11.98	1.60	16.6	1.0	4.4	4.4	129.5
12	<b>Fe4</b>	10	60	30	2500	18.47	2.46	28.7	0.83	4.2	5.1	128.7
13	<b>Fe4</b>	10	70	30	2500	15.90	2.12	27.7	0.91	3.3	3.6	128.7
14	<b>Fe4</b>	10	80	30	2500	10.11	1.35	19.6	0.75	1.4	1.9	125.9
15	<b>Fe4</b>	10	100	30	2500	trace	—	—	—	—	—	—
16	<b>Fe4</b>	10	60	5	2500	6.90	5.52	64.4	0.47	0.66	1.4	126.4
17	<b>Fe4</b>	10	60	10	2500	11.20	4.48	52.3	0.46	1.8	3.8	126.9
18	<b>Fe4</b>	10	60	15	2500	14.42	3.85	44.9	0.76	2.1	2.7	129.2
19	<b>Fe4</b>	10	60	45	2500	22.13	1.96	22.9	0.77	7.8	10	130.2
20	<b>Fe4</b>	10	60	60	2500	24.69	1.65	19.2	0.89	10	11	130.5
21	<b>Fe1</b>	10	60	30	2500	17.35	2.31	26.9	0.56	1.7	3.1	126.4
22	<b>Fe2</b>	10	60	30	2500	7.28	0.97	11.3	0.49	1.4	2.9	126.2
23	<b>Fe3</b>	10	60	30	2500	3.72	0.50	5.83	0.45	1.2	2.6	126.9
24	<b>Fe5</b>	10	60	30	2500	8.40	1.12	13.1	0.48	1.7	3.5	126.7
25	<b>Fe6</b>	10	60	30	2500	trace	—	—	—	—	—	—

<sup>a</sup> General conditions: 1.5 μmol of Fe; 50 mL toluene for 1 atm ethylene, 100 mL toluene for 5 atm and 10 atm ethylene.

<sup>b</sup> 10<sup>6</sup> g mol<sup>-1</sup>(Fe)·h<sup>-1</sup> atm<sup>-1</sup>.

<sup>c</sup> 10<sup>6</sup> g mol<sup>-1</sup>(Fe)·h<sup>-1</sup> C<sup>-1</sup> ethylene.

<sup>d</sup> Determined by GPC.

<sup>e</sup> Determined by DSC.

respectively, and selected bond lengths and angles are shown in Table 2. These complexes (**Fe1**, **Fe2** and **Fe4**) are penta-coordinate with pseudo-square-pyramidal geometry at the metal, with Cl1 occupying the apical position and N1, N2, N3 and Cl2 forming the square plane. The metal center is pressed out of the chelated plane due to the associated sterics: the iron atom lies 0.484 Å out of the chelated plane (N1–N2–N3) in **Fe1**, 0.551 Å in **Fe2** and 0.517 Å in **Fe4**. It is noticeable that the plane of the 2,6-dibenzhydryl-4-chlorophenyl rings is oriented essentially orthogonal to the plane of the bis(imino)pyridine ligand backbone (ranging between 79° and 84°), whereas the angle between the plane of the other aryl ring and the backbone is smaller (ranging between 60° and 70°). Therefore the assumption that the two benzhydryl *ortho*-substituents on the aryl ring can constrain the free rotation of the aryl-nitrogen bond and thus shield the active site, especially at elevated temperatures during the ethylene polymerization, is put forward as a reason for the high observed catalytic activity in the current iron pre-catalysts.

### 3.3. Catalytic behavior toward ethylene polymerization

In order to determine the best co-catalyst to use herein, various alkylaluminum reagents were employed in polymerization runs, and it was found that pre-catalysts treated with modified methylaluminoxane (MMAO) or methylaluminoxane (MAO) produced polyethylene with the highest observed catalytic activities.

#### 3.3.1. Ethylene polymerization with **Fe1–Fe6**/MMAO

The catalytic system of **Fe4**/MMAO was investigated for the optimum catalytic conditions by variation of the molar ratio of Al/Fe, the ethylene pressure, the reaction temperature and the reaction time. Pre-catalysts with different aryl substituents (**Fe1–Fe6**) were then employed in polymerization runs using the optimum

catalytic conditions found for **Fe4**/MMAO. The results, tabulated in Table 2, showed the effects of these parameters on the activities of the pre-catalysts, the molecular weights and the PDIs of the resultant polyethylenes.

Under an ambient pressure of ethylene and with the molar ratio of Al/Fe at 2500, the steady decrease in the catalytic activity of **Fe4** from 0 to 60 °C (Runs 1–4 in Table 3) was the result of the change of the ethylene solubility at elevated reaction temperature. In order to eliminate the influence of ethylene solubility in toluene at different temperatures and various ethylene pressures on the catalytic activity, adjusted activities were introduced, which were obtained

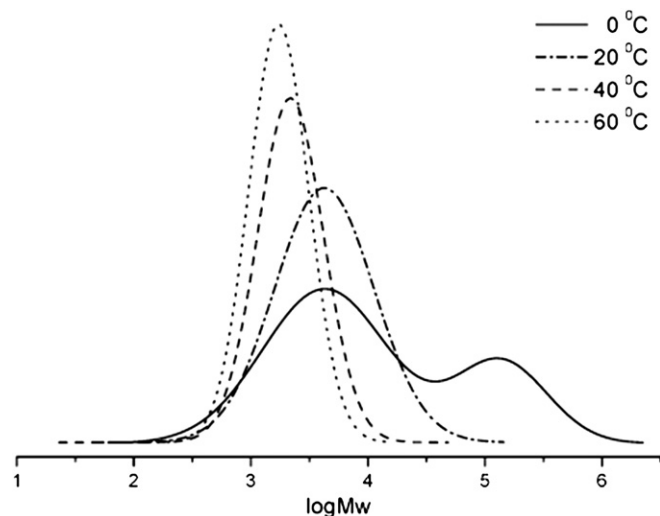


**Fig. 4.** GPC curves of PEs obtained by **Fe4**/MMAO under ambient pressure with various temperatures (Runs 1–4 in Table 3).

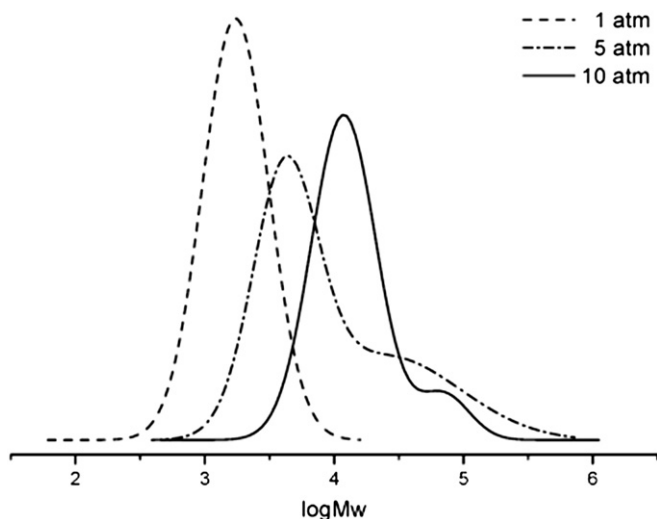


Fig. 5. GPC curves of PEs obtained by **Fe4**/MMAO under various ethylene pressures (Runs 4, 5, 12 in Table 3).

by the calculation such as the linearly decreasing solubility of ethylene about 30% in toluene from 20 °C to 60 °C under 10 atm [48]. Therefore, the best adjusted activity under ambient pressure of ethylene was observed for the catalytic system **Fe4**/MMAO at 40 °C (Run 3 in Table 3). Meanwhile, the GPC curves of the resultant polyethylenes in Fig. 4, which are bimodal at 0 °C and unimodal at higher reaction temperature with a narrow PDI, suggested the dominance of enhanced chain transfer to aluminum [49] at elevated temperature.

Ethylene polymerizations with the catalytic system **Fe4**/MMAO were conducted under different pressures of ethylene (Runs 4, 5, 12 in Table 3). The adjusted catalytic activities increased significantly from  $8.28 \times 10^6 \text{ g mol}^{-1}(\text{Fe}) \text{ h}^{-1} \text{ C}_{\text{ethylene}}^{-1}$  to  $2.87 \times 10^7 \text{ g mol}^{-1}(\text{Fe}) \text{ h}^{-1} \text{ C}_{\text{ethylene}}^{-1}$  on variation of the ethylene pressure, attributable to the higher monomer concentration around the active iron centers at higher pressure. As shown in Table 3 and Fig. 5, the higher the ethylene pressure employed, the greater the molecular weights and PDIs observed for the polyethylene products. It is

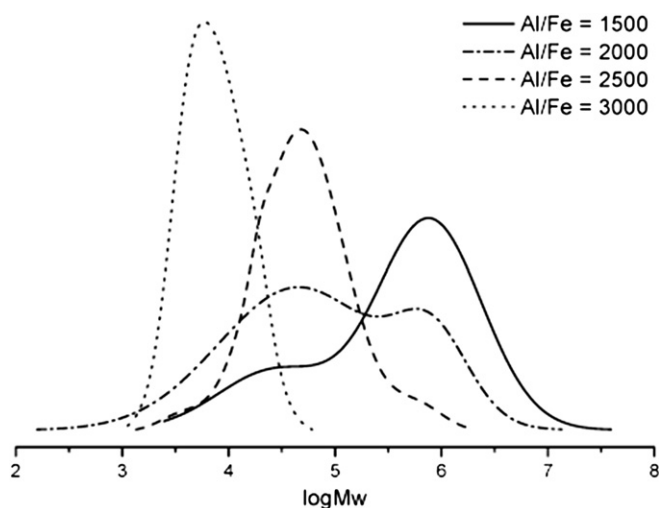


Fig. 6. GPC curves of PEs obtained by **Fe4**/MMAO with various Al/Fe molar ratios (Runs 6–9 in Table 3).

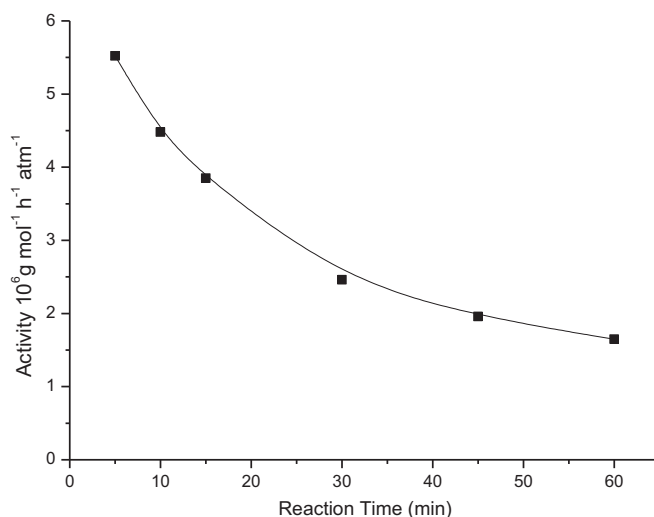


Fig. 7. The effect of the reaction time on the catalytic activity for the **Fe4**/MMAO system (see Runs 12, 16–20 in Table 3).

possible that the higher pressure of ethylene enhanced the rate of chain propagation over the rate of chain transfer. Additionally, precipitated polymeric products could be contributing to the observed bimodal distribution, in particular the peak associated with the higher molecular weights.

Further studies concerning the effect of reaction temperature and ethylene pressure on the active species, and on the pre-catalysts' thermo-stability and catalytic activity were carried out under 10 atm pressure of ethylene. When the Al/Fe molar ratios were raised from 1500 to 3000, the catalytic activities for the **Fe4**/MMAO system at 20 °C initially increased and then decreased (Runs 6–9 in Table 3) with an optimum ratio of 2500 (Run 8 in Table 3). As shown in Fig. 6, the variation of the GPC curves from multi-modal to unimodal suggested that the dominant termination process was chain transfer to aluminum, or simply that as a result of polyethylene precipitation, the equilibrium between the iron and aluminum species responsible for chain transfer was disturbed; similar observations were noted lanthanocene-based systems [50,51].

When the reaction temperature was elevated from 20 to 100 °C (Runs 8, 10–15 in Table 3; 10 atm ethylene, Al/Fe molar ratio 2500:1), the catalytic activity for **Fe4** increased to  $2.46 \times 10^6 \text{ g mol}^{-1}(\text{Fe}) \text{ h}^{-1} \text{ atm}^{-1}$  at 60 °C (Run 12 in Table 3) and then decreased. Although **Fe4** gradually deactivated on increasing the temperature from 60 to 100 °C, the associated lower molecular weights and narrower PDI values were also attributed to the dominance of chain transfer to aluminum at elevated temperature.

The catalytic system **Fe4**/MMAO under 10 atm pressure of ethylene and the Al/Fe molar ratio 2500 at 60 °C was quenched over different reaction periods (Runs 12, 16–20 in Table 3) in order to further understand the lifetime of the active species and the effect of the reaction time on the polymerization behavior. As the reaction time increased from 5 to 60 min, the catalytic activity dropped from  $5.52 \times 10^6 \text{ g mol}^{-1}(\text{Fe}) \text{ h}^{-1} \text{ atm}^{-1}$  to  $1.65 \times 10^6 \text{ g mol}^{-1}(\text{Fe}) \text{ h}^{-1} \text{ atm}^{-1}$ , indicative of little or no induction time during the catalytic process. The effect of reaction time on the catalytic activity is shown in Fig. 7.

Additionally, the PDIs of the resultant polyethylenes (Runs 12, 16–20 in Table 3) varied over different reaction periods, principally relying on the competition between chain propagation and chain transfer. Once the polymeric chains on the active species achieve the requisite length and are ready for the termination stage, this

**Table 4**  
Ethylene polymerization with **Fe1–Fe6**/MAO.<sup>a</sup>

Run	Cat.	T/°C	Al/Fe	Yield/g	Activity <sup>b</sup>	Adjusted activity <sup>c</sup>	M <sub>n</sub> <sup>d</sup> /10 <sup>4</sup> g mol <sup>-1</sup>	M <sub>w</sub> <sup>d</sup> /10 <sup>4</sup> g mol <sup>-1</sup>	M <sub>w</sub> /M <sub>n</sub> <sup>d</sup>	T <sub>m</sub> <sup>e</sup> /°C
1	<b>Fe4</b>	20	1500	1.43	0.19	1.31	1.2	96	80	133.2
2	<b>Fe4</b>	20	2000	1.92	0.26	1.76	0.66	26	40	133.5
3	<b>Fe4</b>	20	2500	2.55	0.34	2.34	0.60	23	38	130.7
4	<b>Fe4</b>	20	3000	2.17	0.29	1.99	0.34	67	20	129.7
5	<b>Fe4</b>	40	2500	5.05	0.67	6.13	0.87	25	29	130.0
6	<b>Fe4</b>	60	2500	5.65	0.75	8.78	1.2	41	3.4	129.5
7	<b>Fe4</b>	70	2500	9.60	1.28	16.7	1.0	2.4	2.4	130.7
8	<b>Fe4</b>	80	2500	10.69	1.43	20.8	0.83	2.3	2.8	130.2
9	<b>Fe4</b>	90	2500	10.20	1.36	21.9	0.70	2.2	3.1	131.0
10	<b>Fe4</b>	100	2500	1.97	0.26	4.65	0.26	0.65	2.5	124.4
11	<b>Fe1</b>	80	2500	9.85	1.31	19.0	1.2	2.0	1.7	130.5
12	<b>Fe2</b>	80	2500	8.40	1.12	16.3	0.95	20	2.1	130.0
13	<b>Fe3</b>	80	2500	2.94	0.32	4.82	0.41	1.1	2.8	128.0
14	<b>Fe5</b>	80	2500	10.30	1.37	19.9	0.68	2.1	3.1	130.5
15	<b>Fe6</b>	80	2500	trace	–	–	–	–	–	–

<sup>a</sup> General conditions: 1.5 μmol of Fe 10 atm ethylene; 100 mL toluene; 30 min.<sup>b</sup> 10<sup>6</sup> g mol<sup>-1</sup>(Fe)·h<sup>-1</sup> atm<sup>-1</sup>.<sup>c</sup> 10<sup>6</sup> g mol<sup>-1</sup>(Fe)·h<sup>-1</sup> C<sup>-1</sup><sub>ethylene</sub>.<sup>d</sup> Determined by GPC.<sup>e</sup> Determined by DSC.

can be achieved by either chain transfer to aluminum [49–51] or via β-H transfer to the ethylene monomer [3,52–54]. On extending the polymerization time, the available amount of MMAO decreased, and chain propagation was more favorable. Such a combination of events resulted in polyethylene products with higher molecular weights and broader molecular distributions.

In the following, all of the pre-catalysts were employed for polymerization under the optimum catalytic conditions found for **Fe4**/MAO (10 atm ethylene, Al/Fe = 2500, 60 °C). All systems exhibited high activities and produced polyethylenes with narrow PDIs. The catalytic activities of the pre-catalysts bearing different substituent's varied in the order **Fe1** [2,6-di(Me)] > **Fe2** [2,6-di(Et)] > **Fe3** [2,6-di(*i*-Pr)] > **Fe6** [2,6-di(Benzhydryl)-4-Cl], **Fe4** [2,4,6-tri(Me)] > **Fe1** [2,6-di(Me)] and **Fe5** [2,6-di(Et)-4-Me] > **Fe2** [2,6-di(Et)] (Runs 12, 21–25 in Table 3 and Runs 8, 11–15 in Table 4), which suggested that a reduction in the steric bulk at the *ortho*-aryl

position and/or replacement of the *para*-aryl proton with a methyl group can increase the activity [1–6]. The highest catalytic activity of these pre-catalysts was obtained by the system **Fe4**/MAO, namely 2.46 × 10<sup>6</sup> g mol<sup>-1</sup>(Fe) h<sup>-1</sup> atm<sup>-1</sup>. Such catalytic activity, and that of the analogous cobalt pre-catalysts [46], is higher than those previously reported by pre-catalysts based on these metals. Thus, given iron pre-catalysts generally show better activities than their cobalt analogs, the current iron pre-catalyst exhibits the highest catalytic activity (as well as good thermal stability) among all iron-based bis(imino)pyridine pre-catalysts reported to-date.

### 3.3.2. Ethylene polymerization with **Fe1–Fe6**/MAO

The catalytic system comprising **Fe4**/MAO was initially employed to determine the optimum catalytic conditions by varying the molar ratios of Al/Fe (Runs 1–4 in Table 4) and the reaction temperature (Runs 5–10 in Table 4). At 10 atm ethylene

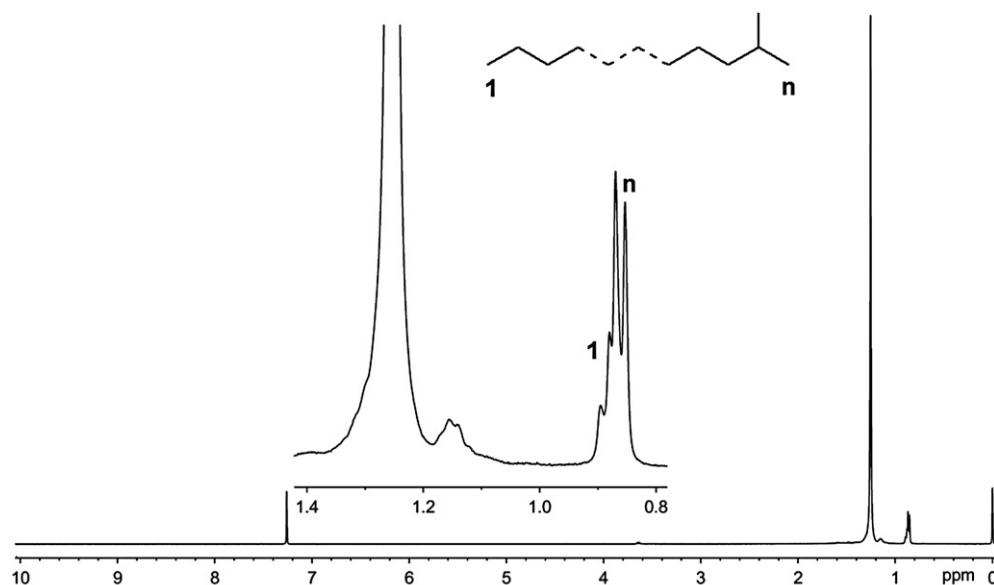


**Fig. 8.** <sup>1</sup>H NMR spectrum of polyethylene prepared with catalyst **Fe4**/MAO (Run 4 in Table 3).

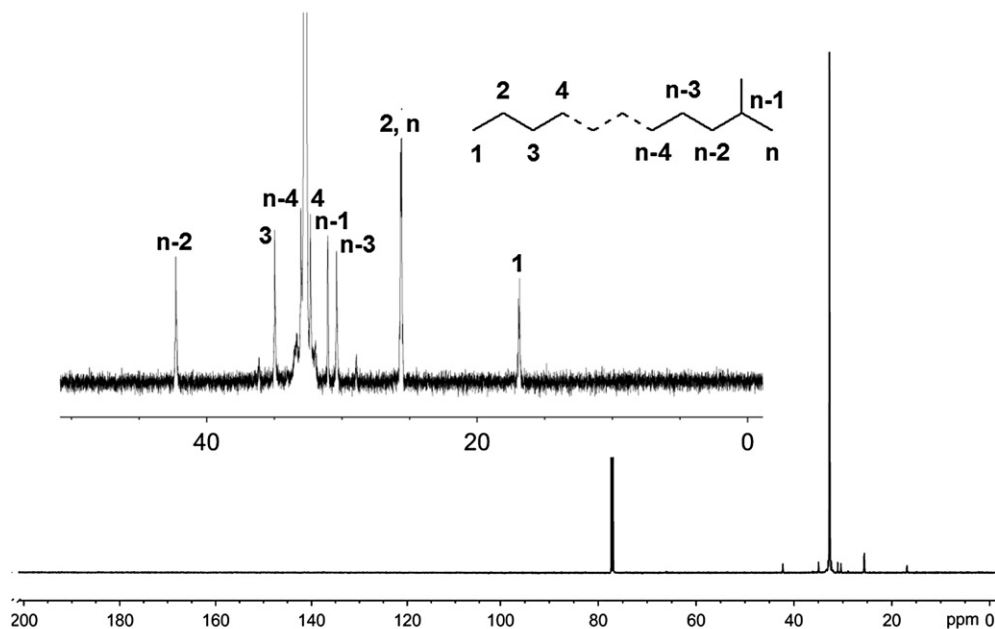


Fig. 9.  $^{13}\text{C}$  NMR spectrum of polyethylene prepared with catalyst **Fe4**/MMAO (Run 4 in Table 3).

pressure, the optimum molar ratio of Al/Fe was 2500 (Run 3 in Table 4), whilst the optimal reaction temperature was  $80\text{ }^\circ\text{C}$  (Run 8 in Table 4). Hence, **Fe4**/MAO exhibited better thermal stability than observed for **Fe4**/MMAO, and produced polyethylene products having narrow molecular weight distributions above  $60\text{ }^\circ\text{C}$  (Run 6 in Table 4).

All of the pre-catalysts were employed for ethylene polymerization under the optimum conditions found using the **Fe4**/MAO system. The order of catalytic activities was similar to that found in the presence of MMAO, namely **Fe1** > **Fe2** > **Fe3** > **Fe6**, **Fe4** > **Fe1** and **Fe5** > **Fe2**. Although the activity was lower, the thermal stability of the **Fe1–Fe5**/MAO catalytic systems was better than those of the **Fe1–Fe5**/MMAO catalytic systems, and the PDIs of the resultant polyethylene products were narrower (1.7–3.1).

In addition, the formation of low molecular weight polyethylene is a consequence of the chain transfer to alkylaluminum [2,4,55–57], which is consistent with the NMR observations on the PE samples. On comparison with the literature [58,59], the analysis of the polyethylene by  $^1\text{H}$  and  $^{13}\text{C}$  NMR spectroscopy clearly showed the absence of signals for olefinic protons and carbons, and thus the products were highly linear polyethylenes, saturated with *i*-propyl end groups when using MMAO (Run 4 in Table 3) as the co-catalyst (Figs. 8 and 9) and with methyl end groups when using MAO (Run 10 in Table 4) as the co-catalyst (Figs. 10 and 11). Under the optimum catalytic conditions of **Fe1–Fe5**/MMAO system and **Fe1–Fe5**/MAO system, chain transfer to aluminum was dominant in the catalytic process; the resultant polyethylenes were of low molecular weight and narrow PDI.

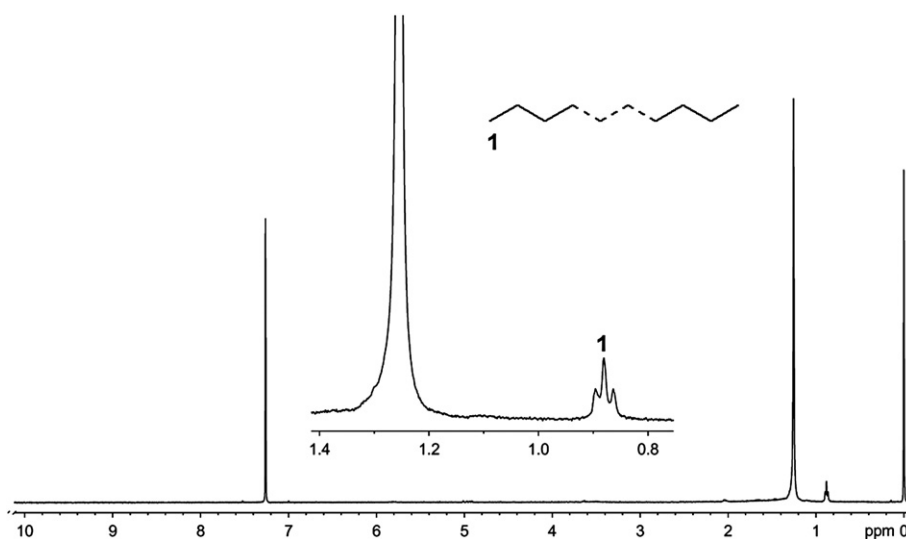


Fig. 10.  $^1\text{H}$  NMR spectrum of polyethylene prepared with catalyst **Fe4**/MAO (Run 10 in Table 4).

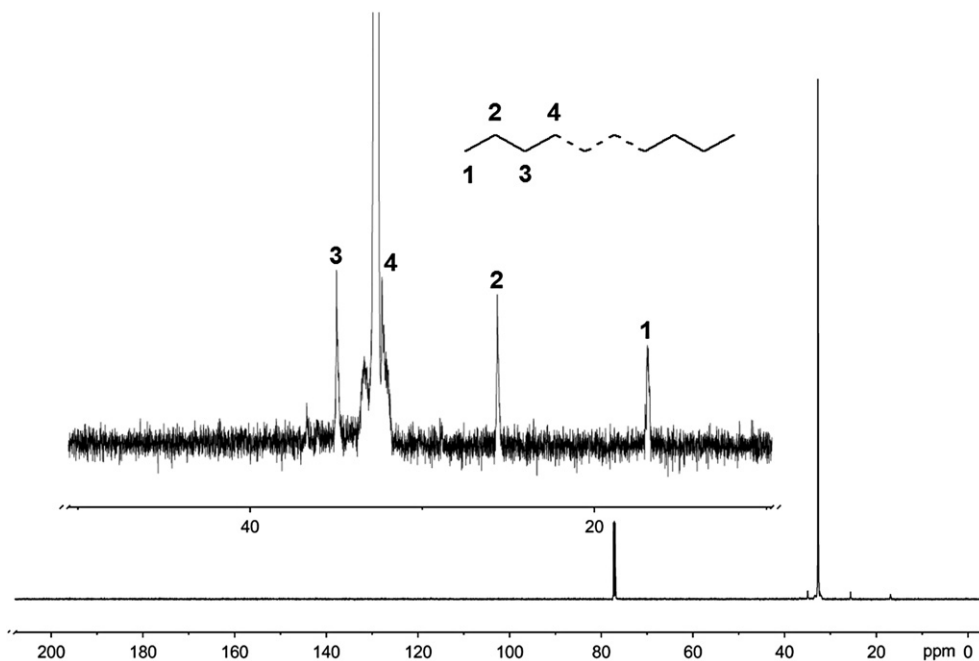


Fig. 11.  $^{13}\text{C}$  NMR spectrum of polyethylene prepared with catalyst **Fe4**/MAO (Run 10 in Table 4).

#### 4. Conclusion

The series of iron(II) complexes (**Fe1–Fe6**) bearing 2-[1-(2,6-dibenzhydryl-4-chlorophenylimino)ethyl]-6-[1-(arylimino)ethyl]pyridine ligands (**L1–L5**) or the ligand 2,6-bis[1-(2,6-dibenzhydryl-4-chloro-phenylimino)ethyl]pyridine (**L6**) were synthesized and fully characterized. On treatment with MMAO or MAO as the co-catalyst, the pre-catalysts (**Fe1–Fe5**) exhibited the highest activity observed for bis(imino)pyridine-based iron systems, with good thermal stability, producing highly linear polyethylene of low molecular weights and with narrow PDIs (single-site active species). Pre-catalysts with such features have the potential to be applied in the industrial production of polyethylene waxes.

#### Acknowledgment

This work is supported by MOST 863 program No. 2009AA034601. CR thanks the EPSRC for an Overseas Travel Grant.

#### Appendix. Supplementary data

Supplementary data associated with this article can be found, in the online version at doi:10.1016/j.polymer.2012.02.050.

#### References

- [1] Small BL, Brookhart M, Bennett AMA. *J Am Chem Soc* 1998;120(16):4049–50.
- [2] Britovsek GJP, Gibson VC, Kimberley BS, Maddox PJ, McTavish SJ, Solan GA, et al. *Chem Commun* 1998;7:849–50.
- [3] Small BL, Brookhart M. *J Am Chem Soc* 1998;120(28):7143–4.
- [4] Britovsek GJP, Bruce M, Gibson VC, Kimberley BS, Maddox PJ, Mastroianni S, et al. *J Am Chem Soc* 1999;121(38):8728–40.
- [5] Small BL, Brookhart M. *Macromolecules* 1999;32(7):2120–30.
- [6] Britovsek GJP, Mastroianni S, Solan GA, Baugh SPD, Redshaw C, Gibson VC, et al. *Chem Eur J* 2000;6(12):2221–31.
- [7] Ma Z, Sun WH, Li Z, Shao C, Hu Y, Li X. *Polym Int* 2002;51(7):994–7.
- [8] Fernandes S, Bellabara RM, Ribeiro AFG, Gomes PT, Ascenso JR, Mano JF, et al. *Polym Int* 2002;51(9):1301–3.
- [9] Bianchini C, Mantovani G, Meli A, Migliacci F, Zanobini F, Laschi F, et al. *Eur J Inorg Chem* 2003;2003(8):1620–31.
- [10] Schmidt R, Welch MB, Knudsen RD, Gottfried S, Alt HG. *J Mol Catal A Chem* 2004;222(1–2):9–15.
- [11] Sun WH, Tang X, Gao T, Wu B, Zhang W, Ma H. *Organometallics* 2004;23(21):5037–47.
- [12] Bianchini C, Giambastiani G, Rios IG, Meli A, Passaglia E, Gragnoli T. *Organometallics* 2004;23(26):6087–9.
- [13] Zhang Z, Chen S, Zhang X, Li H, Ke Y, Lu Y, et al. *J Mol Catal A Chem* 2005;230(1–2):1–8.
- [14] Pelascini F, Wesolek M, Peruch F, Lutz PJ. *Eur J Inorg Chem* 2006;2006(21):4309–16.
- [15] Barbaro P, Bianchini C, Giambastiani G, Rios IG, Meli A, Oberhauser W, et al. *Organometallics* 2007;26(18):4639–51.
- [16] Bianchini C, Giambastiani G, Rios IG, Meli A, Oberhauser W, Sorace L, et al. *Organometallics* 2007;26(20):5066–78.
- [17] Wallenhorst C, Kehr G, Luftmann H, Fröhlich R, Erker G. *Organometallics* 2008;27(24):6547–56.
- [18] Guo L, Gao H, Zhang L, Zhu F, Wu Q. *Organometallics* 2010;29(9):2118–25.
- [19] Sun WH, Hao P, Zhang S, Shi Q, Zuo W, Tang X, et al. *Organometallics* 2007;26(10):2720–34.
- [20] Chen Y, Hao P, Zuo W, Gao K, Sun WH. *J Organomet Chem* 2008;693(10):1829–40.
- [21] Xiao L, Gao R, Zhang M, Li Y, Cao X, Sun WH. *Organometallics* 2009;28(7):2225–33.
- [22] Gao R, Zhang M, Liang T, Wang F, Sun WH. *Organometallics* 2008;27(21):5641–8.
- [23] Gao R, Li Y, Wang F, Sun WH, Bochmann M. *Eur J Inorg Chem* 2009;2009(27):4149–56.
- [24] Sun WH, Hao P, Li G, Zhang S, Wang W, Yi J, et al. *J Organomet Chem* 2007;692(21):4506–18.
- [25] Sun WH, Jie S, Zhang S, Zhang W, Song Y, Ma H, et al. *Organometallics* 2008;25(3):666–77.
- [26] Jie S, Zhang S, Sun WH. *Eur J Inorg Chem* 2007;2007(35):5584–98.
- [27] Zhang M, Zhang W, Xiao T, Xiang JF, Hao X, Sun WH. *J Mol Catal A Chem* 2010;320(1–2):92–6.
- [28] Zhang M, Hao P, Zuo W, Jie S, Sun WH. *J Organomet Chem* 2008;693(3):483–91.
- [29] Zhang M, Gao R, Hao X, Sun WH. *J Organomet Chem* 2008;693(26):3867–77.
- [30] Zhang S, Sun WH, Xiao T, Hao X. *Organometallics* 2010;29(5):1168–73.
- [31] Wang K, Wedeking K, Zuo W, Zhang D, Sun WH. *J Organomet Chem* 2008;693(6):1073–80.
- [32] Xiao T, Zhang S, Li B, Hao X, Redshaw C, Li YS, et al. *Polymer* 2011;52(25):5803–10.
- [33] Xiao T, Zhang S, Kehr G, Hao X, Erker G, Sun WH. *Organometallics* 2011;30(13):3658–65.
- [34] Xiao T, Hao P, Kehr G, Hao X, Erker G, Sun WH. *Organometallics* 2011;30(18):4847–53.
- [35] Song S, Xiao T, Redshaw C, Hao X, Wang F, Sun WH. *J Organomet Chem* 2011;696(13):2594–9.

- [36] Britovsek GJP, Gibson VC, Wass DF. *Angew Chem Int Ed* 1999;38(4):428–47.
- [37] Ittel SD, Johnson LK, Brookhart M. *Chem Rev* 2000;100(4):1169–203.
- [38] Mecking S. *Angew Chem Int Ed* 2001;40(3):534–40.
- [39] Gibson VC, Spitzmesser SK. *Chem Rev* 2003;103(1):283–315.
- [40] Bianchini C, Giambastiani G, Rios IG, Mantovani G, Meli A, Segarra AM. *Coord Chem Rev* 2006;250(11–12):1391–418.
- [41] Gibson VC, Redshaw C, Solan GA. *Chem Rev* 2007;107(5):1745–76.
- [42] Bianchini C, Giambastiani G, Luconi L, Meli A. *Coord Chem Rev* 2010;254(5–6):431–55.
- [43] Yu J, Liu H, Zhang W, Hao X, Sun WH. *Chem Commun* 2011;47(11):3257–9.
- [44] Yu J, Huang W, Wang L, Redshaw C, Sun WH. *Dalton Trans* 2011;40(39):10209–14.
- [45] Zhao W, Yu J, Song S, Liu H, Hao X, Redshaw C, et al. *Polymer* 2012;53(1):130–7.
- [46] Lai J, Zhao W, Yang W, Redshaw C, Liang T, Liu Y, et al. *Polym Chem* 2012;3(3):787–93.
- [47] Sheldrick GM. SHELXL-97, program for the refinement of crystal structures. Germany: University of Göttingen; 1997.
- [48] Krauss W, Gestrich W. *CZ-Chem-Tech* 1977;6(12):513–6.
- [49] Kempe R. *Chem Eur J* 2007;13(10):2765–73.
- [50] Pelletier JF, Mortreux A, Olonde X, Bujadoux K. *Angew Chem Int Ed Engl* 1996;35(16):1854–6.
- [51] Chenal T, Olonde X, Pelletier JF, Bujadoux K, Mortreux A. *Polymer* 2007;48(7):1844–56.
- [52] Barabanov AA, Bukatov GD, Zakharov VA, Semikolenova NV, Echevskaja LG, Matsko MA. *Macromol Chem Phys* 2005;206(22):2292–8.
- [53] Barabanov AA, Bukatov GD, Zakharov VA, Semikolenova NV, Mikenas TB, Echevskaja LG, et al. *Macromol Chem Phys* 2006;207(15):1368–75.
- [54] Kissin YV, Qian C, Xie G, Chen Y. *J Polym Sci A Polym Chem* 2006;44(21):6159–70.
- [55] Wang S, Liu D, Huang R, Zhang Y, Mao B. *J Mol Catal A Chem* 2006;245(1–2):122–31.
- [56] Tomov AK, Gibson VC, Britovsek GJP, Long RJ, Meurs M, Jones DJ, et al. *Organometallics* 2009;28(24):7033–40.
- [57] Haas I, Kretschmer WP, Kempe R. *Organometallics* 2011;30(18):4854–61.
- [58] Galland GB, Souza RF, Mauler RS, Nunes FF. *Macromolecules* 1999;32(5):1620–5.
- [59] Galland GB, Quijada R, Rojas R, Bazan G, Komon ZJA. *Macromolecules* 2002;35(2):339–45.